KeAi
CHINESE ROOTS
GLOBAL IMPACT

Available online at www.sciencedirect.com

ScienceDirect

Green Energy & Environment 8 (2023) 1325–1340

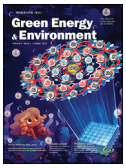

www.keaipublishing.com/gee

Review article

Prelithiation strategies for silicon-based anode in high energy density lithium-ion battery

Tianqi Jia [a,b], Geng Zhong [a,b], Yao Lv [c], Nanrui Li [a,b], Yanru Liu [a,b], Xiaoliang Yu [d], Jinshuo Zou [e], Zhen Chen [a], Lele Peng [a], Feiyu Kang [a,b,*], Yidan Cao [a,b,*]

[a] *Shenzhen Geim Graphene Center, Institute of Materials Research, Shenzhen International Graduate School, Tsinghua University, Shenzhen, 518055, China*
[b] *Tsinghua-Berkeley Shenzhen Institute, Tsinghua University, Shenzhen, 518055, China*
[c] *College of Sciences and Institute for Sustainable Energy, Shanghai University, Shanhai, 200000, China*
[d] *Department of Mechanical Engineering, The Hong Kong Polytechnic University, Hong Kong, 999077, China*
[e] *School of Chemical Engineering & Advanced Materials, The University of Adelaide, Adelaide, SA 5005, Australia*

Received 4 May 2022; revised 7 August 2022; accepted 17 August 2022
Available online 24 August 2022

Abstract

Green energy storage devices play vital roles in reducing fossil fuel emissions and achieving carbon neutrality by 2050. Growing markets for portable electronics and electric vehicles create tremendous demand for advanced lithium-ion batteries (LIBs) with high power and energy density, and novel electrode material with high capacity and energy density is one of the keys to next-generation LIBs. Silicon-based materials, with high specific capacity, abundant natural resources, high-level safety and environmental friendliness, are quite promising alternative anode materials. However, significant volume expansion and redundant side reactions with electrolytes lead to active lithium loss and decreased coulombic efficiency (CE) of silicon-based material, which hinders the commercial application of silicon-based anode. Prelithiation, pre-embedding extra lithium ions in the electrodes, is a promising approach to replenish the lithium loss during cycling. Recent progress on pre-lithiation strategies for silicon-based anode, including electrochemical method, chemical method, direct contact method, and active material method, and their practical potentials are reviewed and prospected here. The development of advanced Si-based material and prelithiation technologies is expected to provide promising approaches for the large-scale application of silicon-based materials.

Keywords: Si-based materials; Prelithiation; Coulombic efficiency; Lithium loss; Lithium-ion battery

1. Introduction

In the era of carbon emission deduction, electric vehicles and green energy storage devices have become hot topics [1–5]. Since the commercialization in 1991, rechargeable lithium-ion battery (LIB) has achieved great success and is currently one of the most widely used electrochemical energy storage systems in portable devices and electric vehicles due to the small self-discharge, high energy density, long cycle life, high operating voltage, no memory effect and environmental friendliness [6–9]. Generally, the commercial LIBs consist of graphite as anode, layered transition metal oxides (e.g. $LiCoO_2$) or olivine type (e.g. $LiFePO_4$) materials as cathode, and lithium ion-containing ester-based electrolyte. Growing markets for portable electronics and electric vehicles create tremendous demand for advanced lithium ion batteries (LIBs) with high power and energy density. However, conventional graphite anode materials cannot meet such increasing demand due to their limited capacity. Alternative anode materials, such as silicon-based materials [10–12], tin-based materials [13–

* Corresponding authors.
E-mail addresses: fykang@sz.tsinghua.edu.cn (F. Kang), yidancao@sz.tsinghua.edu.cn (Y. Cao).

https://doi.org/10.1016/j.gee.2022.08.005

15], and alloy materials [16–18], etc., have attracted numerous research activities. Silicon, which has the high theoretical gravimetric capacity of 3579 mAh g^{-1} and volumetric capacity of 2194 Ah L^{-1}, several times higher than the conventional graphite counterpart (372 mAh g^{-1}, 719 Ah L^{-1}) [19–22], is one of the most promising alternatives and widely investigated in both academia and industry. Silicon also possesses other desirable qualities, as shown in Fig. 1 [23]. Silicon (Si) is the second most abundant element in the earth crust, which provides an excellent opportunity to reduce the cost of batteries (on a per Ah basis). The low electrochemical potential and environmental benign of silicon make it possible to develop safe devices with high energy density [24].

A key challenge for the application of Si is the vast volume expansion (~280%) during its lithiation [25,26], which leads to the disruption of the passivation layer on the lithiated Si surface (i.e. solid electrolyte interphase (SEI)), increased surface exposure, continuous electrolyte consumption due to newly formed SEI, particle pulverization, and material detachment from current collector, etc. (Fig. 2) [27–31]. As a result, there is severe lithium loss, and the initial coulombic efficiency (ICE) as well as the CE during cycling of Si are much lower than those of graphite. Low ICE and CE would be detrimental to the cycling performance, especially in full cells where silicon-based anode is paired with a cathode with only limited amount of lithium. Extensive work, such as synthesis of alloy/composite materials [32–35], controlling particle sizes/microstructures/nanostructures [36–39], and design of surface coatings [40–43], have been carried out to deal with the mentioned problems and improve the cyclability of silicon. The application of pure silicon is still challenging in spite of all these trials [44,45]. Meanwhile, the SiO_x material has attracted much attention as a trade-off between capacity and cyclability in recent years. SiO_x has a high capacity of ~1000–2500 mAh g^{-1} (depending on the x value) [46], relatively low volume expansion of <150% and extended cycle life with special microstructure engineering [47]. However, the low initial coulombic efficiency (ICE) of SiO_x materials is one of the main drawbacks when used as anode materials in Li-ion batteries, which consumes lithium ions shuttling between cathode and anode and cut down the energy density of the battery [48]. Prelithiation of anode, the basic principle of which is adding lithium-containing material to the anode material in advance to compensate for the lithium loss during the initial cycles, is an effective way to improve the CE and cyclability [49–54].

During the past years, prelithiation has attracted increasing attentions to improve the cycling durability of silicon-based materials. This review first illustrates the origins/mechanisms of initial lithium loss in Si-based anode materials and demonstrates the necessity of prelithiation in section 2. Recent progress on prelithiation approaches for silicon-based anodes is reviewed in section 3. Finally, challenges and perspectives for future prelithiation technologies and their practical potentials are prospected in section 4.

2. Lithium loss and necessity of prelithiation

The coulombic efficiencies (CE) in the initial and first several cycles are lower than the stable CE, i.e. the delithiation capacity is much lower than the lithiation capacity, suggesting that some lithium ions are lost and the shuttling lithium ions between cathode and anode are reduced [55]. There are several reasons for the lithium loss and low CEs in silicon-based anode materials, including lithium loss originated from SEI, lithium loss from volumetric changes of silicon-based materials and lithium loss at defect sites in the anode materials [56].

2.1. Lithium loss originated from SEI

The commonly used electrolyte is thermodynamically unstable at low potential on a negatively polarized anode surface, and interfacial reactions between anode and electrolyte as well as electrolyte (solvents and lithium salts) decomposition occur irreversibly [57]. As a result, solid electrolyte interphase (SEI) layer is formed, and the SEI formation process consumes lithium ions. SEI consists of organic (e.g. lithium ethylene dicarbonate (LEDC, $(CH_2OCO_2Li)_2$, polycarbonates, etc.), and inorganic (e.g. LiF, Li_xO, Li_2CO_3, etc.) compounds [58,59]. The components and microstructure of SEI are dependent on the electrode/electrolyte interface, which makes it very complicated. For example, in the case of Si anode in the ester-based electrolyte, the inorganic components in the SEI are adjacent to the negative electrode, while the organic components are adjacent to the electrolyte after the initial reduction during the first cycle, as shown in Fig. 3a. The components in the organic layer, such as LEDC, are not stable and can dissolve into the electrolyte. The decomposition and dissolution of unstable components would repeat for continuous cycling until more stable components form, and the Li-ion-consumption will also last until stable SEI forms (Fig. 3a–b) [57,60,61].

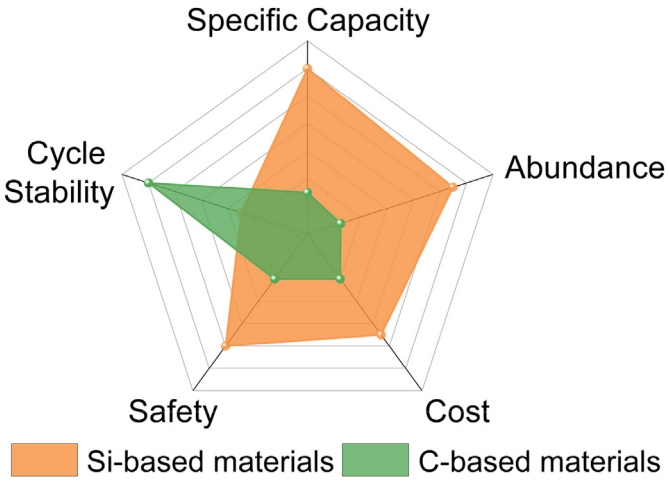

Fig. 1. The performance comparison of Si-based and C-based anode materials.

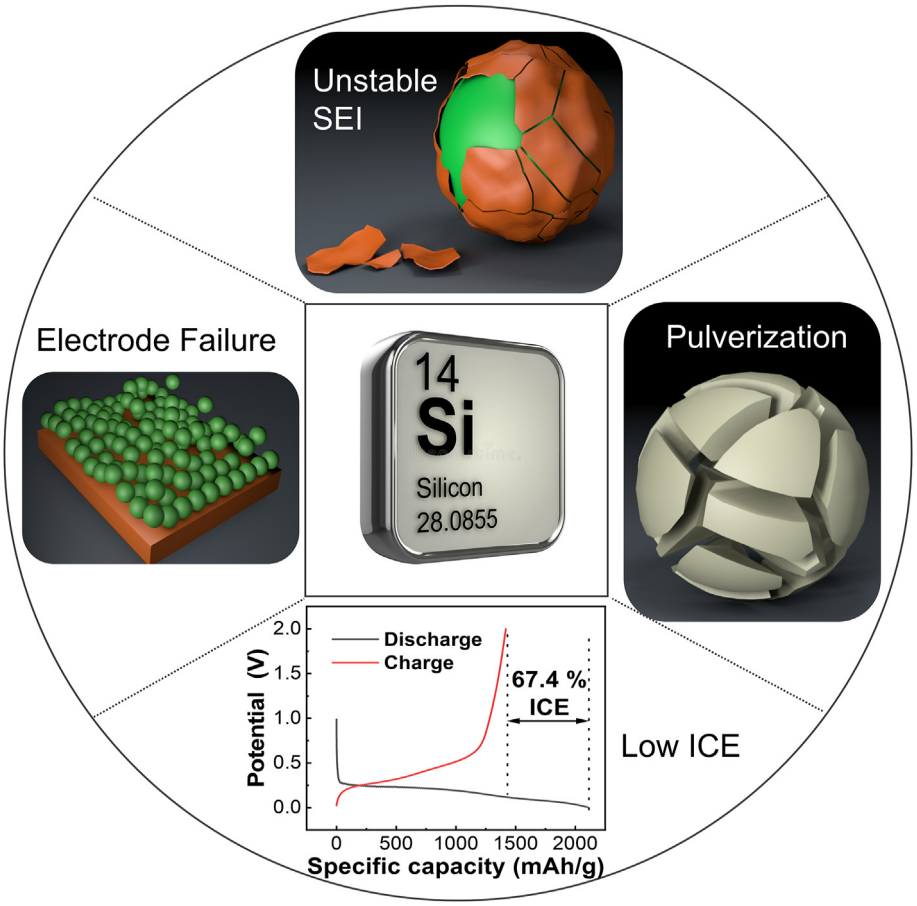

Fig. 2. Main demerits of Si-based anode material.

2.2. Lithium loss from volumetric changes

During lithiation, $Li_{15}Si_4$ alloy forms, and the anode will suffer from an extraordinary expansion of ~280%, which results in lithium loss from diffusion-controlled lithium trapping and dead lithium in ruptured/detached particles [62,63]. During the first cycle, lithium ions diffuse into the electrode during the lithiation step, whereas the lithium concentration at the electrode surface decreases during the subsequent delithiation step, which gives rise to an intermediate region in which the lithium concentration is higher than those both at the surface and in the interior parts. The lithium can then diffuse both towards the electrode surface and further into the electrode, i.e. two-ways. Lithium may diffuse too far into the electrode to be recovered within the time domain of the subsequent delithiation step, and a small part of the deposited lithium ions therefore are trapped in the electrode on each cycle. Recent studies indicate that the effect of Li trapping in Si anodes accounts for approximately 30% of the initial Li loss for the first cycle and leads to accelerated decay of Si anode capacity in the subsequent cycles [64,65]. Thus, minimizing Li trapping is critical to avoid lithium loss and improve the initial CE of Si anodes. For example, Zhu et al. [63] demonstrate that by introducing Ge substitution in Si with fine compositional control, the energy barrier of lithium diffusion will be significantly reduced because of the lattice expansion (Fig. 3c). On the other hand, active Si-based material particles and their surrounding matrix would crack or even pulverize under the stress of large volume change during cycling, which will lead to the breakdown of the conductive network formed by the conductive carbon and current collector, and a sharp increase of the internal resistance. As a result, the delithiation would not be completed for the disconnected particles with some inaccessible lithium. Even worse, new surfaces created by particle ruptures will react with the electrolyte continuously, form new SEI layers, and consume active lithium ions (Fig. 3d) [66,67].

2.3. Lithium loss at defect sites

The lithiation/delithiation in the active materials is theoretically reversible. However, some lithium ions may not be able to delithiate after the first lithiation due to the formation of highly stable lithiated compounds or strong bonding with atoms at defect sites. High amounts of defects are expected at the interfaces and grain boundaries, especially in Si-based alloy particles [52]. A large amount of Li is stored on the defects or heteroatoms, which cannot be released again, resulting in the vast Li loss and low ICE. Irreversible reactions between lithium and reactive oxygen are another source for

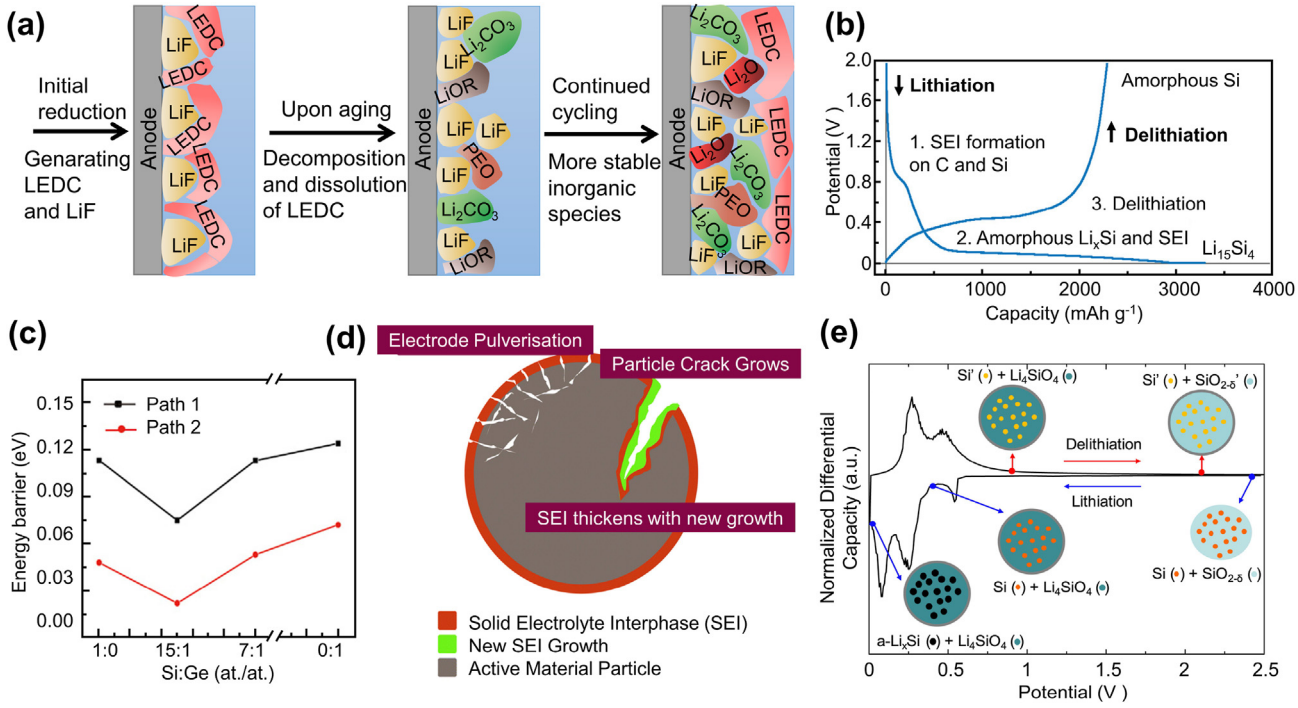

Fig. 3. (a) The formation process of solid electrolyte interphase (SEI) layer in a silicon-based anode. Reprinted with permission from Ref. [57]. Copyright (2019) Elsevier. (b) Voltage curves of C/Si anode material in the first cycle. Reprinted with permission from Ref. [60]. Copyright (2015) American Chemical Society. (c) Energy barrier of lithium diffusion in Ge modified silicon with various Si:Ge ratios. Path 1 is related to free Li atom which does not form an equilateral triangle with other Li atoms and migrates to an equilateral triangle vacancy with two Li atoms. Three Li atoms are the vertices of an equilateral triangle. Path 2 is that the Li atom in the fully occupied equilateral triangle migrates to other equilateral triangle vacancy with two Li atoms. Reprinted with permission from Ref. [63]. Copyright (2019) American Association for the Advancement of Science. (d) Schematic of lithium loss during silicon electrode failure. Reprinted with permission from Ref. [67]. Copyright (2021) Royal Society of Chemistry. (e) Differential capacity curve and corresponding changes of SiO_x anode in the process of the initial lithiation/delithiation. Reprinted with permission from Ref. [47]. Copyright (2020) IOP science.

lithium loss, although the by-products may enhance the conductivity of the Si-based electrode. Typically, in SiO_x or other oxygen-containing material, the formation of Li_4SiO_4 matrix may occur before the formation of $Li_{15}Si_4$ (Fig. 3e) [22,47]. Delithiation of these compounds occurs at relatively high voltage, which exceeds the typical cycling range of lithium ion battery [47]. As a result, these parts of lithium ions are irreversible, which leads to irreversible capacity and low initial coulombic efficiency. However, inactive matrix like Li_4SiO_4 is able to suppress volume expansion of active silicon through mechanical stress and facilitate lithium-ion conductivity, which can significantly reduce the volume changes and avoid the above-mentioned mechanical failure. Therefore, a method that can maintain the beneficial matrix as well as improve ICE is highly desired.

2.4. The necessity of prelithiation

All these lithium losses occur in the initial several cycles, and the ICE of Si-based materials is way lower than that of the commercial graphite even though strategies like innovated electrolytes have been reported [63,68–71]. This difference would be detrimental to the specific energy density of the full cell consisting of a silicon-based anode and a positive electrode with limited lithium amount. Lithium sources are initially stored in the cathode for a full cell, and the low ICE of the anode would require additional Li source to compensate for the Li losses due to the formation of SEI, particle rupture and lithium trappings, etc. As a result, the amount of shuttling lithium ions would be greatly reduced, i.e. the capacity and energy density would drop. Let's take a typical NMC||SiO system, which consists of NMC as the cathode (200 mAh g^{-1}) and SiO as the anode (2000 mAh g^{-1}) with an average voltage of 3.8 V, as an example. The energy density (Energy Density = Cell Capacity × Average Voltage) would be 691 Wh kg^{-1} if the ICE is 100%, and the energy density would drop to 484 Wh kg^{-1} if the ICE of SiO is 70%. Therefore, a promising approach, named prelithiation, by pre-embedding lithium ions in the anode material to replenish the lithium loss is effective in alleviating this issue, so that the amount of active lithium ions in the battery can be kept at a high level in the full cell. Homogeneous and stable SEI layer can also be established on purpose by prelithiation. Henceforth, severe fracture and pulverization of Si-based particles and excessive side reactions between anode and electrolyte would be avoided, resulting in improved energy density of full cells. Various strategies have been proposed and tested to prelithiate Si-based anode, which will be reviewed in the following section. These findings and progress provide significant guidance to the practical application of Si-based

anode. However, it is still challenging to seek for highly efficient, economical, and industrially practical prelithiation method.

3. Prelithiation approaches for silicon-based anodes

The prelithiation of anode materials mainly includes electrochemical, chemical, direct contact and active material assisted prelithiation methods.

3.1. Electrochemical prelithiation

Electrochemical prelithiation is a widely studied method for prelithiation. There are two forms of setups, including galvanic cell and electrolytic cell, for electrochemical prelithiation. The galvanic cell, also called voltaic cell, utilizes an external short circuit between the metallic lithium and the active electrode separated by the separator soaked in the electrolyte [72]. An optimized circuit resistance and simultaneously monitoring the voltage between both electrodes are required to control the prelithiation process [73]. By contrast, galvanostatic current is applied to the electrolytic cell to initiate the chemical reactions, in which Li^+ ions from lithium source (Li metal, electrolyte, etc) embed in the working electrode with active materials until a cut-off voltage is achieved [74]. The lithiation accuracy in both setups is easy to control by simply changing the applied resistance/current and time, and the setups for both methods are simple and convenient to realize on lab scale. Although the prelithiation level can be precisely regulated, additional procedures including the disassembly of cells and the subsequent reassembly are needed prior to the normal charge–discharge process.

The galvanic cell, which consists of lithium foil, active electrodes and resistances in the external circuit, has been utilized for controlled prelithiation. Kim et al. [73] introduced a scalable but delicate prelithiation scheme for silicon monoxide (c-SiO_x) by short circuiting active electrodes with lithium metal foil, in which the degree of prelithiation can be fine-tuned to improve the performance of SiO_x in full cell. The overall prelithiation was processed in a closed coin cell assembly (Fig. 4a). Spontaneous prelithiation was initiated by the potential difference between both electrodes as soon as an external short circuit was constructed between c-SiO_x electrode and lithium metal foil in the presence of electrolyte and separator in between. Lithium plating and dendrites formation will occur if the material is overlithiated (ICE>100%), which will puncture the separator, cause short circuit, destroy the original SEI and result in the continuous consumption of electrolyte and Li^+ due to new SEI formation. Otherwise, the ICE will not be effectively improved if underlithiated. A resistor was included in the external short circuit to control the speed of prelithiation, and the end point of the prelithiation was determined by the cell voltage monitored throughout the prelithiation. 100 Ω and 30 min were selected for fine control of prelithiation to achieve both reasonable lithiation time and cell voltage, and avoid overlithiation/underlithiation (Fig. 4b–c). If the resistance was more than 100 Ω, the lithiation time would be too long. In contrast, if the resistance was lower than 100 Ω, the voltage was too low to measure accurately (Fig. 4b). When the prelithiation time was 40 min, the ICE was 107.9%, indicating an overlithiation (Fig. 4c). 30 min was proper, and CEs of the first three cycles reached 94.9%, 95.7% and 97.2%, respectively, leading to a full cell (pairing SiO_x with the nickel-rich layered cathode, $Li[Ni_{0.8}Co_{0.15}Al_{0.05}]O_2$) energy density 1.5-times higher than that of graphite-$LiCoO_2$ counterpart. Although this strategy is relatively simple and controllable, the complex assembling and disassembling operations as well as extra usage of lithium metal and electrolytes result in an expensive fabrication, which impedes its practical application. In addition, the prelithiation process is moisture sensitive and requires moisture-free atmosphere in scalable fabrication.

In order to reduce the consumption of lithium metal and alleviate uncontrollable safety issues, Zhou et al. [74] reported a novel electrolytic cell to prelithiate Si electrode in a well-controlled way without the usage of Li metal. As shown in Fig. 4d, the electrolytic cell consisted of Cu wire counter electrode in the aqueous Li_2SO_4 electrolyte and a silicon working electrode in a gel polymer electrolyte. Lithium ions for prelithiation were from the lithium salt in the electrolyte. The reaction of the electrolytic cell was: $xLi^+ + \frac{x}{2}Cu + Si = Li_ySi + (x - y)Li + \frac{x}{2}Cu^{2+}$. This Li-metal-free method, with high controllability, no short circuiting and abundant Li source in aqueous solution, resulted in a high specific energy density up to 349 Wh kg^{-1} and 732 Wh kg^{-1} when the lithiated silicon anode was paired with MnO_x and S in a full cell, respectively (Fig. 4e). Moreover, the only byproduct $CuSO_4$ can be easily recycled and the manufacture of the electrolytic cell parts is accessible. Without the use of Li metal or complex surface chemistry of Li metal, this electrolytic cell provides a safe and green way to realize powerful Li-ion batteries by prelithiation. Similarly, Guo et al. [75] found that anti-perovskite type Li_2OHCl, a solid-state Li^+ conductor, can be electrolyzed at 3.3 V or 4 V to release O_2, HCl and Li^+ via decomposition routes, depending on the acidity of electrolyte. The electrolysis of Li_2OHCl delivered a lithium releasing capacity up to 810 mAh g^{-1}, and the released Li ions effectively prelithiated Si/C composite anode to enhance the energy density of full cells. The Li_2OHCl is also a potential prelithiation lithium reservoir considering that the exhausted HCl can be reused to regenerate Li_2OHCl in a sustainable cycle.

Overhoff et al. [76] used a Swagelok-type Si/C||Li metal cell, consisting of Si/C electrodes as working electrode, Li metal foil as counter and reference electrode and a polyolefin separator wetted with electrolyte, to prelithiate Si/C electrode in constant current (2000 mA g^{-1}) mode to a potential of 0.02 V vs. $Li|Li^+$. The result showed that the open circuit potential (OCP) of the Si/C electrode was significantly reduced (Fig. 4f). After prelithiation, a layer of SEI was formed on the electrode in advance and the volume of the Si particles expanded in a controlled way, which effectively

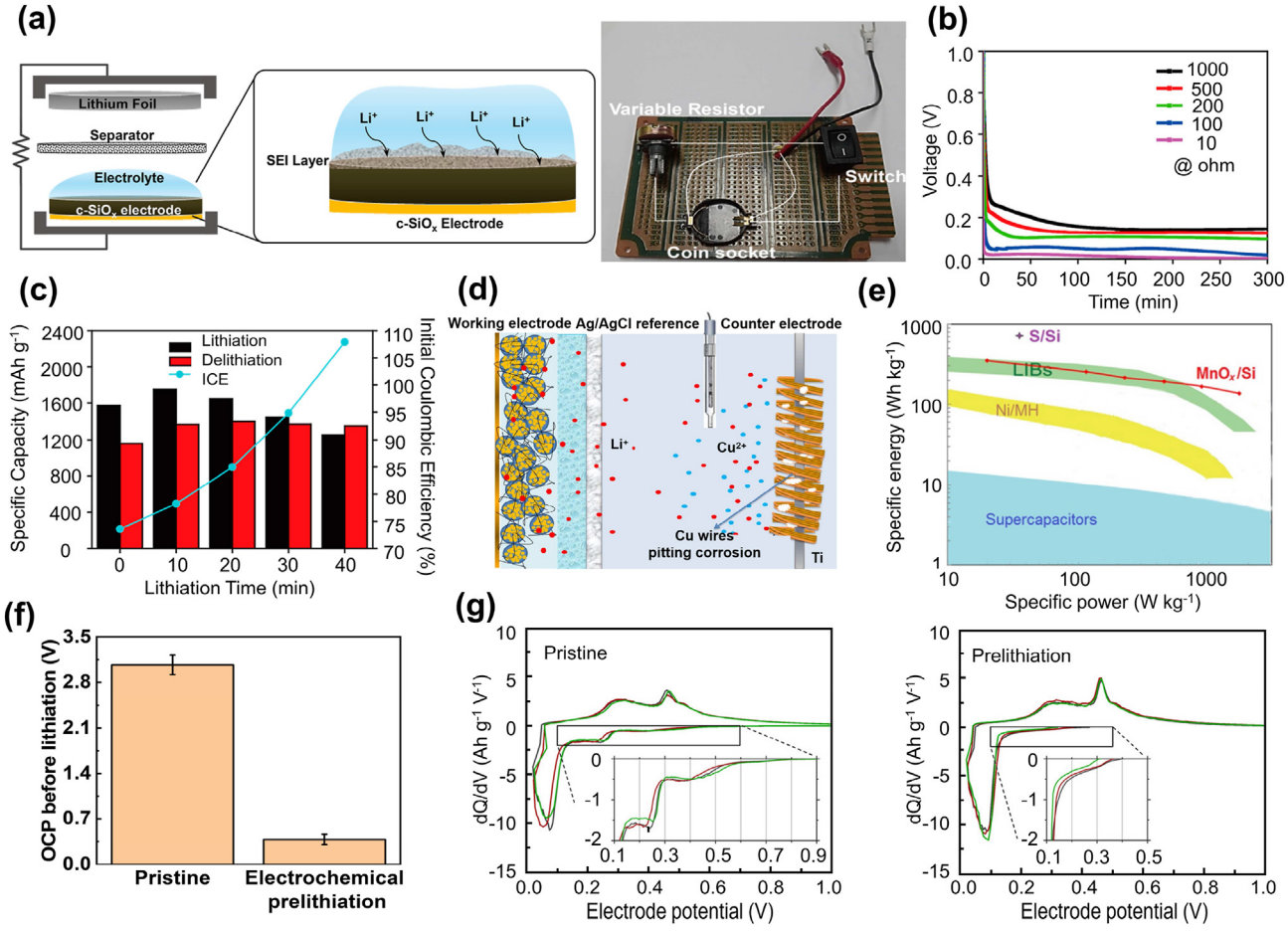

Fig. 4. (a) Schematic of the internal structure and external circuit of galvanic cell for controlled prelithiation of SiOx anode. Reprinted with permission from Ref. [73]. (b) The effect of external resistance on cell voltage. Reprinted with permission from Ref. [73]. Copyright (2016) American Chemical Society. (c) Dependence of specific capacity and initial coulombic efficiency (ICE) on prelithiation time. Reprinted with permission from Ref. [73]. Copyright (2016) American Chemical Society. (d) Schematic of the internal structure of electrolytic cell consisting of Cu wires in aqueous Li_2SO_4 and Si electrodes in a gel polymer electrolyte. Reprinted with permission from Ref. [74]. Copyright (2015) John Wiley and Sons. (e) Specific energy and power density of MnOx/Si and S/Si full cells using prelithiated Si anode, Li-ion batteries (LIBs), Ni/MH batteries, and supercapacitors. Reprinted with permission from Ref. [74]. Copyright (2015) John Wiley and Sons. (f) Open circuit potential (OCP) of pristine Si/C electrode and Si/C electrode after electrochemical prelithiation. Reprinted with permission from Ref. [76]. Copyright (2021) John Wiley and Sons. (g) Differential capacity (dQ/dV) curves of pristine Si/C electrode and Si/C electrode after electrochemical prelithiation. The three colors represent duplicated cells. Reprinted with permission from Ref. [76]. Copyright (2021) John Wiley and Sons.

suppressed cracks formation during cycling. As shown in Fig. 4g, differences between prelithiated and pristine electrodes were detected during the beginning of lithiation. The lithiation-process differential capacity curve of pristine electrode started to increase around 0.90 V, having one broad plateau down to 0.30 V and an additional peak at 0.25 V. The initial increase at high potential was induced by decomposition of the electrolyte solvents as well as of the additive or the conducting salt $LiPF_6$ to form the SEI [77]. In contrast, the prelithiated electrodes showed less differential capacity increase and showed up at lower potentials, indicating an already formed protective SEI layer and partial lithiation of the active material during pre-lithiation. After prelithiation, ICE was increased from 69% to 83%. This method is highly feasible in lab-scale, however, also requires extra lithium, electrolyte, dis- and re-assembling, which is not practical in large-scale manufacture.

Prelithiation by electrochemical method is a widely used method for prelithiation study in research labs. However, most of the methods need an additional process of disassembly and reassembly for batteries and a long prelithiation time, hindering their practical application. Besides, there are potential risks of safety issues, such as lithium plating and thermal runaway due to the high reactivity of metallic lithium. As prelithiation is considered as additional manufacturing step during cell production, prelithiation by electrolysis (electrochemical bath) approach seems to be one of the most promising strategies among electrochemical methods, since it avoids usage of highly reactive lithium metal and reactive salts, uses low-cost Li salts as Li source, and realizes homogeneous prelithiation in solution. Further studies focusing on improving electrochemical prelithiation technology, including shortening prelithiation time, improving stability of SEI, realizing prelithiation in a more controllable way, etc., are still

highly desired to improve energy density and long-term cycling performance of LIBs.

3.2. Direct contact methods

Another strategy to realize prelithiation is to directly enable the contact between lithium metal and the active anode material in the electrolyte. Electric field is formed immediately due to the potential difference between the anode material and lithium metal, and the electrons will move from the low potential region to the high potential region at the point of contact under the action of the electric field. In order to remain electrically neutral, the Li metal will release lithium ions which pass through the electrolyte and embed into the anode material to complete the lithiation process. Both lithium metal foil and lithium metal powder have been used for direct contact prelithiation. The setups of direct contact method utilize the self-discharge of either lithium metal foil or powder, which are relatively simple and efficient. However, the unevenly distributed contact points between lithium and electrode always leads to inhomogeneous prelithiation. In addition, it is challenging to control the degree of prelithiation, and the removal of residual lithium metal adds extra step/cost for manufacture.

3.2.1. Direct contact with lithium foil

As shown in Fig. 5a, the transfer of Li^+ and electrons between the Li foil and the electrode material occurs only at the contact points and radiates at the interface due to the rough surface texture, resulting in partial concentrated Li^+ flux/diffusion and uneven prelithiation of the electrode. Additionally, the strong reduction property of metallic lithium also induces a highly inhomegeneous prelithiation in the perpendicular direction of the interface plan. Buffer interfacial layer, high pressure, and engineered nanostructures have been reported in order to deal with the uneven prelithiation problems due to the uneven contact between silicon-based materials and lithium metal.

Meng et al. [78] placed a flexible resistance buffer layer (RBL), consisting of poly(vinyl butyral) (PVB) coated carbon nanotube film, with good electrical conductivity between the SiO_x negative electrode and lithium metal (Fig. 5b). PVB with excellent plasticity enabled an excellent contact with metallic lithium and electrode. At the same time, carbon nanotube film had remarkable conductivity, and the resistance of the RBL can be controlled by PVB. As a result, adding RBL turned out to be a reliable approach to alleviate nonuniform electron transfer and facilitate homogeneous prelithiation. As shown in Fig. 5c, with this RBL layer, the distributions of Li and C were more uniform in the RBL modified case, indicating more homogeneous prelithiation. Stable SEI was formed and there were no microcracks or fractured powder on the surface of silicon-based materials. The initial coulombic efficiency was increased from 68.9% to 87.3% after prelithiation, and that of full cell was increased from 68% to 87%. After 200 cycles, the capacity retention of the NCM622||SiO_x full cell was 74% with the capacity of 128 mAh g^{-1} after prelithiation, which is much superior to 66 mAh g^{-1} of the full cell without prelithiation (Fig. 5d). A tri-layer structure of active material/polymer (PMMA)/lithium anode, which is stable in ambient air (10–30% relative humidity) for a period that is sufficient to manufacture anode materials, has been reported to buffer the interface between the Li metal and active material. The polymer layer can protect lithium metal foil from O_2 and moisture, and it gradually dissolved in the electrolyte, then active materials contacted with lithium to form lithiated anode (Fig. 5e) [79]. The polymer layer in the tri-layer structure not only rendered electrodes stable in ambient air but also led to uniform prelithiation of silicon-based anodes.

Applying high pressure onto Li metal foil-Si/C contact to enable sufficient contact is an effective way to realize prelithiation via direct contact [76,80]. Yao C et al. [80] enhanced the initial coulombic efficiency of Si wrapped by graphene oxide nanoribbons (GONPs) electrode to 97.1% by direct contact Li metal under 1 kg cm^{-1} pressure in an argon atmosphere for several minutes. The prelithiated Si-GONPs showed superior cycle stability with specific capacities of 1235 mAh g^{-1} at 1000 mA g^{-1} and 969 mAh g^{-1} at 2000 mA g^{-1} after 500 cycles, respectively. Shi L et al. [81] improved the safety of Li ion sulfur battery by replacing lithium metal with the high-pressure prelithiated SiO_x/C negative electrode, and this kind of cell showed a high reversible capacity of 616 mAh g^{-1} after 100 cycles and a high energy density of 661 Wh kg^{-1} which is 2 times than that of lithium-ion battery. Nanostructures as well as high pressure were applied to introduce more contact points for prelithiation. Silicon nanowires (SiNW) were grown on a stainless steel (SS) substrate (Fig. 5f) and pressure was applied to induce electrical contact and lithiation between SiNWs and Li foil [82]. The nano-structured Si possessed three main merits: (1) efficient 1D electron transport, (2) good contact with the current collector, (3) facile stress relaxation. After prelithiation, the structure of the silicon nanowires remained unchanged. As shown in Fig. 5g, SEI and alloy layers formed by this method were similar to those in-situ formed during cycling. The silicon nanowires can be ~50% lithiated after 20 min and 100% lithiated after 60 min of prelithiation, respectively (Fig. 5h). However, there is a tradeoff between lithiated lithium amount and cyclability, and 20 min is an optimized period for prelithiation in this case. Watanabe T et al. [83] improved direct contact method by using laminated cells composed of through-holed cathodes and anodes with diameters of 20, 100, and 200 μm. They found that the irreversible capacity was significantly reduced by optimizing the prelithiated charge amount, capacity balancing time and the hole diameter. Shellikeri A et al. [84] studied the effect of different Li resources (lithium metal powder, thick Li strip, thin Li film, thin Li film with pin holes) on prelithiation and indicated that the anode potential vs. Li/Li^+ was the lowest by using Li strips and there was little influence on prelithiation by pin holes.

Compared with methods related to high pressure and engineered nanostructures to deal with uneven prelithiation, the prelithiated electrodes are more uniform by buffer interfacial layers. Buffer interfacial layer is the most efficient and

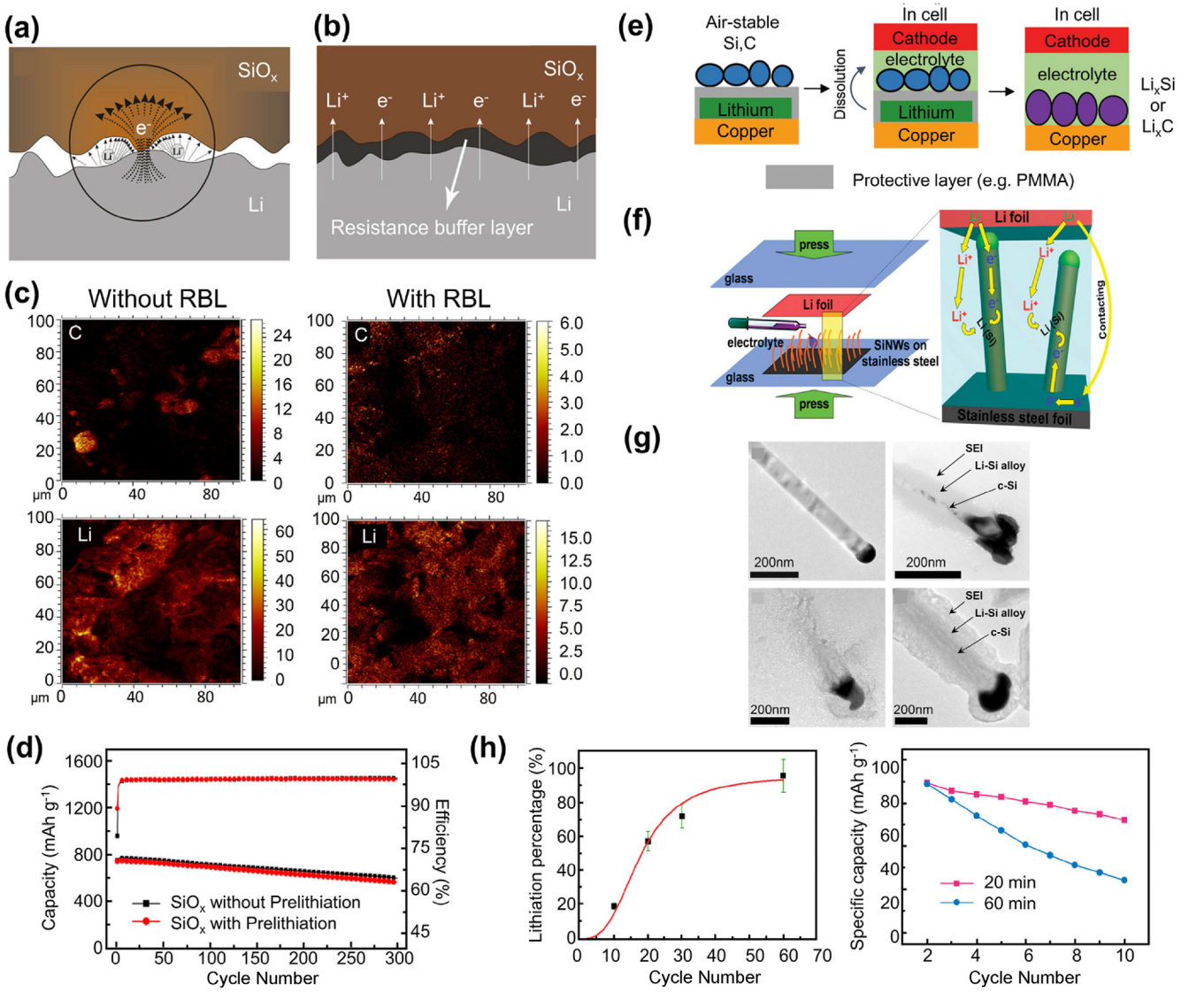

Fig. 5. (a) The principle of direct contact method. Reprinted with permission from Ref. [78]. Copyright (2019) American Chemical Society. (b) Direct contact prelithiation process regulated by flexible resistance buffer layer (RBL). Reprinted with permission from Ref. [78]. Copyright (2019) American Chemical Society. (c) Distribution of carbon (C) and lithium (Li) on the electrode surface without RBL and with RBL, respectively. Reprinted with permission from Ref. [78]. Copyright (2019) American Chemical Society. (d) Specific capacity and Coulombic efficiency of NCM622-SiOx battery with and without prelithiation. Reprinted with permission from Ref. [78]. Copyright (2019) American Chemical Society (e) Schematic of the role of polymer layer (e.g. PMMA) protecting lithium metal foil and the process of prelithiation in cell. Reprinted with permission from Ref. [79]. Copyright (2016) American Chemical Society. (f) The process of pre-lithiating silicon nanowires (SiNWs) grown on a stainless steel (SS) substrate. Reprinted with permission from Ref. [82]. Copyright (2011) American Chemical Society. (g) TEM images showing the structure of a pristine SiNW (upper left), a 10 min prelithiated SiNW (upper right), a 20 min prelithiated SiNW (lower left) and a ~50% electrochemically lithiated SiNW by using 0.5C constant current for 10 h (lower right). Reprinted with permission from Ref. [82]. Copyright (2011) American Chemical Society. (h) The dependence of prelithiation percentage on prelithiation time (left). The role of the red line is just for eye guidance. Cycling performance of 20 min prelithiated SiNWs and 60 min prelithiated SiNWs (right). The first cycle is hidden for clarity. Reprinted with permission from Ref. [82]. Copyright (2011) American Chemical Society.

can be easily manipulated to essentially improve the prelitiation homogeneity. For instance, when silicon-based materials were prelithiated for fixed time, the efficiency with buffer interfacial layer was close to 140%, which is way higher than those under high pressure (~110%) and engineered nanostructures (<60%) [78,82,85]. Nevertheless, high pressure is the most convenient one among three strategies. Overall, it is convenient and effective to realize the prelithiation by direct contact with lithium foil method, which is appropriate for the production of industrialized electrode. Additionally, this method can achieve a large degree of prelithiation in a few minutes for high energy density LIBs. In the meantime, compared with more active lithium power, lithium foils are safer for the practical use in laboratory/industry. However, the contact points at the interface are limited by the surface quality of the electrode and the lithium foil due to the face-to-face contact configuration. The degree of prelithiation is uneven since prelithiation preferentially occurs at the contact

points. Further increase of the number of contact points during prelithiation by direct contacting with lithium foil is still needed to realize the homogeneous prelithiated electrodes, elevate the energy density of LIBs and promote the cycling life.

3.2.2. Direct contact with lithium metal powder

An important strategy to improve interfacial contact between lithium metal and electrode material is to use lithium metal powder for prelithiation, but lithium-metal powder is very reactive and explosive in the air. Stabilized lithium metal powder (SLMP) has been introduced by FMC Corporation and Jarvis et al. to avoid safety issues during prelithiation [86]. The size of SLMP particles ranges from several micrometers to hundred micrometers, which can be safely handled in dry air. The improved stability is related to a thin Li_2CO_3 protective layer around Li metal particles (Fig. 6a) [87,88]. The high capacity of SLMP can compensate the initial lithium loss during a prelithiation process, which can take the place of the long and tedious electrically charged formation cycle in Li-ion battery manufacture for cost saving. However, the handling and application of SLMP on the anode is still challenging. The protective layer needs to be broken down by pressure to expose reactive Li and enable electrical contact before SLMP can be used for prelithiation [89,90], which is called activation of SLMP. A safer, less expensive and scalable process to disperse SLMP in anode is also highly desired. There are different ways to carry out prelithiation with SLMP. SLMP can be introduced to the battery system by two different methods, i.e. surface coating and slurry mixture. The surface application method is realized by coating SLMP to the surface of a prefabricated electrode sheet. Among surface application

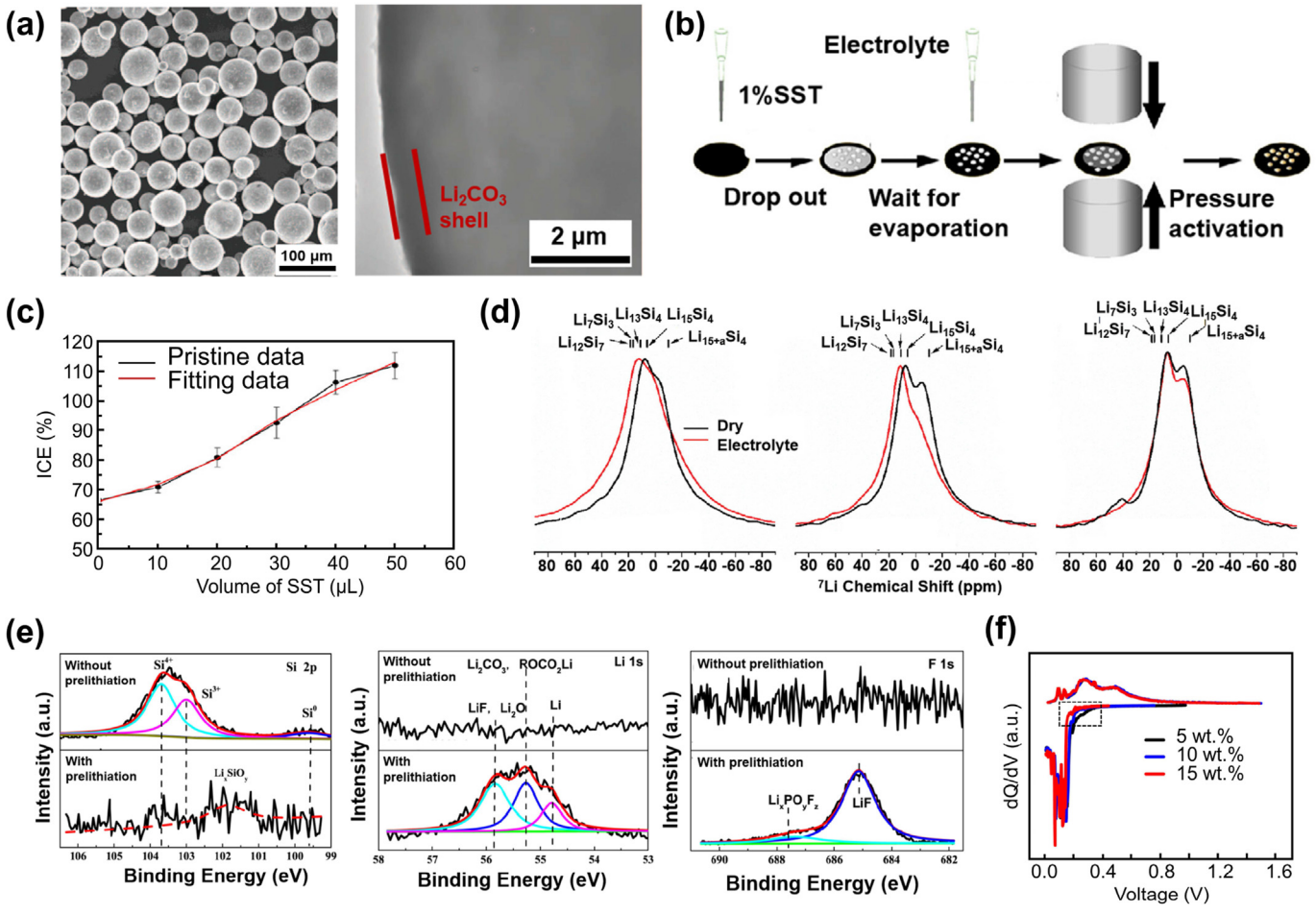

Fig. 6. (a) SEM images of stabilized lithium metal powder (SLMP) and the surface Li_2CO_3 protective layer. Reprinted with permission from Ref. [88]. Copyright (2013) IOPscience. (b) Schematic of the prelithiation process of SiO electrode using the suspension (SST) consisting of stabilized lithium metal powder (SLMP), styrene butadiene rubber (SBR) and toluene. Reprinted with permission from Ref. [97]. Copyright (2021) American Chemical Society. (c) Dependence of ICE on the volume of the suspension (SST). The red curve shows that ICE increases linearly as the suspension (SST) volume increases. Reprinted with permission from Ref. [97]. Copyright (2021) American Chemical Society. (d) Ex-situ solid-state ^{7}Li nuclear magnetic resonance (NMR) analyses of silicon/graphite electrodes in dependence on the degree of prelithiation using stabilized lithium metal powder (SLMP). Analyses of 25% prelithiated silicon/graphite electrode (left), 50% prelithiated silicon/graphite electrode (middle), 75% prelithiated silicon/graphite electrode (right) in the dry state for 24 h without electrolyte (black curve) and in the wet state for additional 48 h with electrolyte (red curve). Reprinted with permission from Ref. [101]. Copyright (2021) John Wiley and Sons. (e) XPS spectra of Si 2p, Li 1s, F 1s of SiO/Graphite/Carbon electrodes with and without prelithiation. Reprinted with permission from Ref. [89]. Copyright (2017) Elsevier. (f) Differential capacity (dQ/dV) curves of the prelithated SiO/Graphite/Carbon electrodes with 5 wt%, 10 wt%, 15 wt% SLMP. Reprinted with permission from Ref. [89]. Copyright (2017) Elsevier.

approaches, spraying is a generally used method with high potential for large-scale fabrication in the manufacturing process. The slurry application method involves the mixing of SLMP particles with the active anode material, conductive agent and polymer binder to formulate a slurry mixture which is then cast on the current collector [91]. However, SLMP is not compatible with the common used solvents for electrode fabrication, including N-methyl pyrrolidinone (NMP), dimethyl acetamide (DMA), and dimethyl formamide (DMF), and can only be dispersed in nonpolar solvents, like hexane or toluene.

Spray approach has been shown to be effective for SLMP, and a surfactant needs to be added to improve SLMP dispersion [92–94]. SLMP has been dispersed in toluene/hexane, which then could be homogeneously applied on the surface of the electrode [6,95]. The powder was roll pressed onto the surface of the electrode when toluene was evaporated. Subsequently the electrode was pressurized to break Li_2CO_3 protective layer and to induce reaction between the lithium and the silicon-based material. Zhao et al. [92] successfully increased the ICE of SiO from 48% to ~90% with the SLMP and enabled the NMC/SiO full cell to maintain a reversible capacity of ~110 mAh g^{-1} after more than 100 cycles at C/3. Forney et al. [96] utilized SLMP to effectively prelithiate high capacity (1500–2500 mAh g^{-1}) silicon−carbon nanotube (Si-CNT) anodes, eliminating 20–40% of the initial irreversible capacity loss. The prelithiation approach enabled high energy density NCA/Si-CNT batteries achieving >1000 cycles at 20% depth of discharge. However, using SLMP-toluene as the prelithiation reagent is not ideal, because it is an unstable suspension that must be shook or stirred during use. Huang et al. [97] added SLMP into mixed styrene butadiene rubber (SBR) and toluene to form suspension followed by droping the suspension (SST) onto the SiO electrode and activating SLMP by pressure to complete the process of prelithiation (Fig. 6b). Initial coulombic efficiency was elevated from 66% to 75–120% at an optimized pressure of 20 MPa, which could be easily controlled by adjusting the volume of SST (Fig. 6c). The prelithiation of biomass-derived silicon/carbon composite materials was carried out in a similar way by dispersing SLMP in xylene solution composed of poly(styrene-co-butadiene) rubber (SBR) and polystyrene (PS) [98]. The ICE of the pretreated materials was increased from 72% to 95.1%. Besides spray coating method, other approaches, including slurry mixture with SLMP, dry coating, etc., have been proposed for prelithiation. SLMP was added into electrode slurry for film casting with SBR binder [99]. Yao K et al. [100] directly pressed the SLMP powder onto the surface of freestanding flexible Si nanoparticles–multiwalled carbon nanotubes (SiNPs–MWNTs) composite paper anode in a dry room to avoid the use of toxic solvents such as xylene and toluene. After prelithiation, the active lithium loss was successfully reduced from 806 to 28 mAh g^{-1} and the ICE was increased from 65% to 98%.

Prelithiation by SLMP can effectively improve the ICE and compensate the lithium loss during cycling, which is revealed to be correlated with the formation of stable SEI. However, the homogeneity of prelithiation as well as the homogeneity of SEI is not well controlled. Bärmann et al. [101] unraveled the prelithiation mechanism of silicon-graphite electrode in dependence of the degree of prelithiation by SLMP direct contact method in either “dry state” (SLMP was added in the dry state onto the electrode, pressed and rested for 24 h) or “wet state” (additional contact to electrolyte for 48 h after the dry state). The lithiation of electrode occurred in the dry state, with no necessity to add electrolyte to initiate lithiation. However, this process occurred from particle lateral and was very inhomogeneous. Lithium distribution became more homogeneous and lithiation continued more peripheral from the SLMP after electrolyte addition, leading to a more homogeneous SEI layer. In addition, the bulk composition of electrode was quite dependent on the prelithiation process (SLMP amount, time, dry or wet). As shown in Fig. 6d, ex situ ^7Li nuclear magnetic resonance (NMR) studies proved that direct contact prelithiation occurred only between contact points. There was a broad ^7Li signal at ~7.5 ppm in the dry state, indicating the formation of highly lithiated phase $Li_{15}Si_4$. With the growing of prelithiation degree, overlithiated phase $Li_{15+a}Si_4$ at ~-6 ppm appeared, which further suggested the presence of $Li_{15}Si_4$ phase. After adding electrolyte, a small shoulder appeared at ~-0.8 ppm, which was related to the formation of SEI after the lithiated electrodes contacted with electrolyte. Additionally, ^7Li signal at ~7.5 ppm shifted to ~11.5 ppm, which related to the transformation from $Li_{15}Si_4$ to $Li_{13}Si_4$. The above phenomena did not appear in 75% highly prelithiated electrode, which indicated that SEI has been formed before adding electrolyte. Pan et al. [89] added lithium metal powder to hexane (toluene or xylene) to form a suspension, then added the suspended droplets to the silicon surface and applied pressure to carry out the prelithiation on SiO-based composite electrode. The surface chemistry after prelithiation was carefully analyzed by XPS (Fig. 6e). After prelithiation, the peaks assigned to Si^{4+} and Si^0 disappeared, suggesting that SiO either reacted with SLMP or was covered by the SEI produced in the prelithiation reaction. One weak peak at 102.0 eV was detected in the Si2p profile, which was attributed to the formation of Li_xSiO_y, the product of the irreversible reaction between SiO and lithium. Moreover, LiF rich SEI was detected after prelithiation. As a result, the degree of prelithiation was accurately controlled by 5 wt%, 10 wt% and 15 wt% SLMP addition to reduce the irreversible lithium consumption at ~0.2–0.5 V during the first cycle (Fig. 6f) and improve ICE to 74.4%, 85.0% and 98.5%, respectively.

Direct contact method by lithium metal is a promising strategy, especially prelithiation by SLMP. The degree of prelithiation can be controlled with high accuracy with SLMP in comparison to prelithiation with Li metal foil. Also, it is unnecessary to remove the SLMP prior to cell assembly since the Li metal is dissolved thoroughly prior to real battery cell operation in the optimal case. However, SLMP is considerably much more expensive, and the inhomogeneous distribution of SLPM within the electrode may lead to safety issues, non-uniform SEI formation and unintentional aging behavior.

These are still challenging before SLMP can be large-scale applied in practical manufacture. Besides, there is still a lack of understanding on the mechanism of SEI-formation, lithiation chemistry, and aging behavior during the prelithiation process, which would be highly demanded to further optimize the prelithiation strategy.

3.3. Active materials assisted prelithiation method

Li-containing solid reagent materials, which can react with the inactive components in the electrode to eliminate the active lithium loss, can also be used to compensate for active lithium loss during initial cycles.

This method has been used for SiO_x materials to compensate for the lithium loss due to the formation of lithium silicates. Veluchamy et al. [102] thermal treated LiOH and SiO mixture at 550 °C and observed the presence of Li_4SiO_4 particles which can effectively improve ICE as well as facilitate Li^+ diffusion. Zhao et al. [103] reported an excellent prelithiation reagent Li_xSi–Li_2O core–shell nanoparticle, which was prepared by a one-step thermal alloying process between Li and Si nanoparticle, for both silicon and graphite (Fig. 7a). The nano-sized silicon particles and lithium metal were mixed and heated to form Li_xSi alloy followed by a treatment in dry air to get the final core–shell structure with Li_xSi covered by Li_2O. The potential of Li_xSi–Li_2O was only 10 mV higher than that of lithium metal, and it had a high specific capacity of 2000 mAh g^{-1}. The initial lithium loss was greatly reduced and the corresponding coulombic efficiency of Si anode was increased from 74% to 94% by this reagent (Fig. 7b). However, as shown in Fig. 7c, Li_xSi–Li_2O core–shell NPs are only compatible with 1,3-dioxolane (DOL) and toluene to extract the capacity, but not compatible with the traditional solvent *N*-methyl-2-pyrrolidone(NMP) or diethyl carbonate (DEC), which hinders the commercial application Li_xSi–Li_2O. Additionally, the chemical stability of this reagent still needs to be further improved for practical use, since exposure to moisture will cause the significant capacity drop of it. In order to deal with the above mentioned capacity decay of Li_xSi active material after a period of time in air [103]. Zhao et al. [104] established a layer of LiF and lithium alkyl carbonate with long hydrophobic carbon chains on the surface of the Li_xSi through a reaction process similar to SEI formation, according to Eqs. (1) and (2).

$$F\text{-}(CH_2)_9CH_3 + Li_xSi \rightarrow LiF + Li\text{-}(CH_2)_9CH_3 \quad (1)$$

$$Li\text{-}(CH_2)_9CH_3 + O_2/CO_2 \rightarrow Li\text{-}OC(=O)O\text{-}(CH_2)_9CH_3 \quad (2)$$

The chemical stability and moisture resistance were greatly improved by the modification layer (Fig. 7d). Both alloying and intercalation anode materials can be effectively prelithiated with the coated Li_xSi reagent to counteract the initial lithium loss.

Some other reactive precursors have also been used to induce the prelithiation and improve ICE of silicon-based anodes. Zhu et al. [105] prelithiated $Si@SiO_x$ negative electrode using $LiBH_4$ to generate $Si@Li_2SiO_3$ finally (Fig. 7e). As shown in Fig. 7f, initial conlumbic efficiency was increased from 66.5% to 89.1%. However, the whole process needs to be carried out in the glove box since $LiBH_4$ is very explosive when heated in the air. Chung et al. [106] developed a Li metal-free dehydrogenation-driven prelithiation method employing lithium hydride (LiH) to react with SiO and produce irreversible Li_2O and Li_2SiO_3, as shown below Ep. (3) and (4). Lithium from LiH served as a source for the preemptive formation of lithium silicate phases which are the primary origin of the poor ICE of SiO. The obtained three-dimensionally networked Si/lithium silicate nanocomposites (Fig. 7g) could improve the ICE of SiO up to 90.5%.

$$1.5Si + 1.5SiO_2 + 2LiH \rightarrow 2Si + SiO_2 + 2Li_2O + 2H_2\ (g) \quad (3)$$

$$SiO_2 + Li_2O \rightarrow Li_2SiO_3 \quad (4)$$

Active material assisted prelithiation is highly efficient and the process is easy to handle. However, the common reagents are usually active and could react with water, oxygen and carbon dioxide in the air. It is challenging to find an appropriate prelithiation reagent, which is not only chemical stable in air but also compatible with the components in the battery (binder, solvents, electrolytes, etc.).

3.4. Chemical prelithiation

The lithium metal can be dissolved together with biphenyl (BP)/naphthalene (NP) in organic solvents like butyl methyl ether (DME) or tetrahydrofuran (THF), resulting in the formation of radical anions paired with lithium ions. The Li-containing solution is very stable in the air. The electrons of the radical anions and lithium ions are transferred to the electrode material when putting the electrode into the solution, recovering the initial state of the radical anions and resulting in embedded lithium ions in the electrode. This process depends on the low redox potential of the solute. Therefore, it is key to seek appropriate solutes for specific silicon-based anodes considering the low electrochemical potential of silicon vs. Li/Li^+.

The first investigation on reducing active lithium loss by chemical prelithiation was based on negative electrodes reacting with n-butyl lithium (n-BuLi) prior to cell construction [107]. Later on, this chemical method was used on SiO material by immersing it in Li-organic complex solution obtained by dissolving naphthalene and metallic Li into butyl methyl ether (BME) solvent to improve its ICE. Shen et al. [108] also used lithium naphthalide to improve the initial coulombic efficiency of silicon anode to 93.5% (Fig. 8a). Yan et al. [109] used lithium-biphenyl (Li-BP) in tetrahydrofuran (THF) solution to react with SiO_x/C material, and then calcined the powders at high temperature to get homogeneous prelithiation. Li_xSiO_y was formed inside the SiO_x/C material,

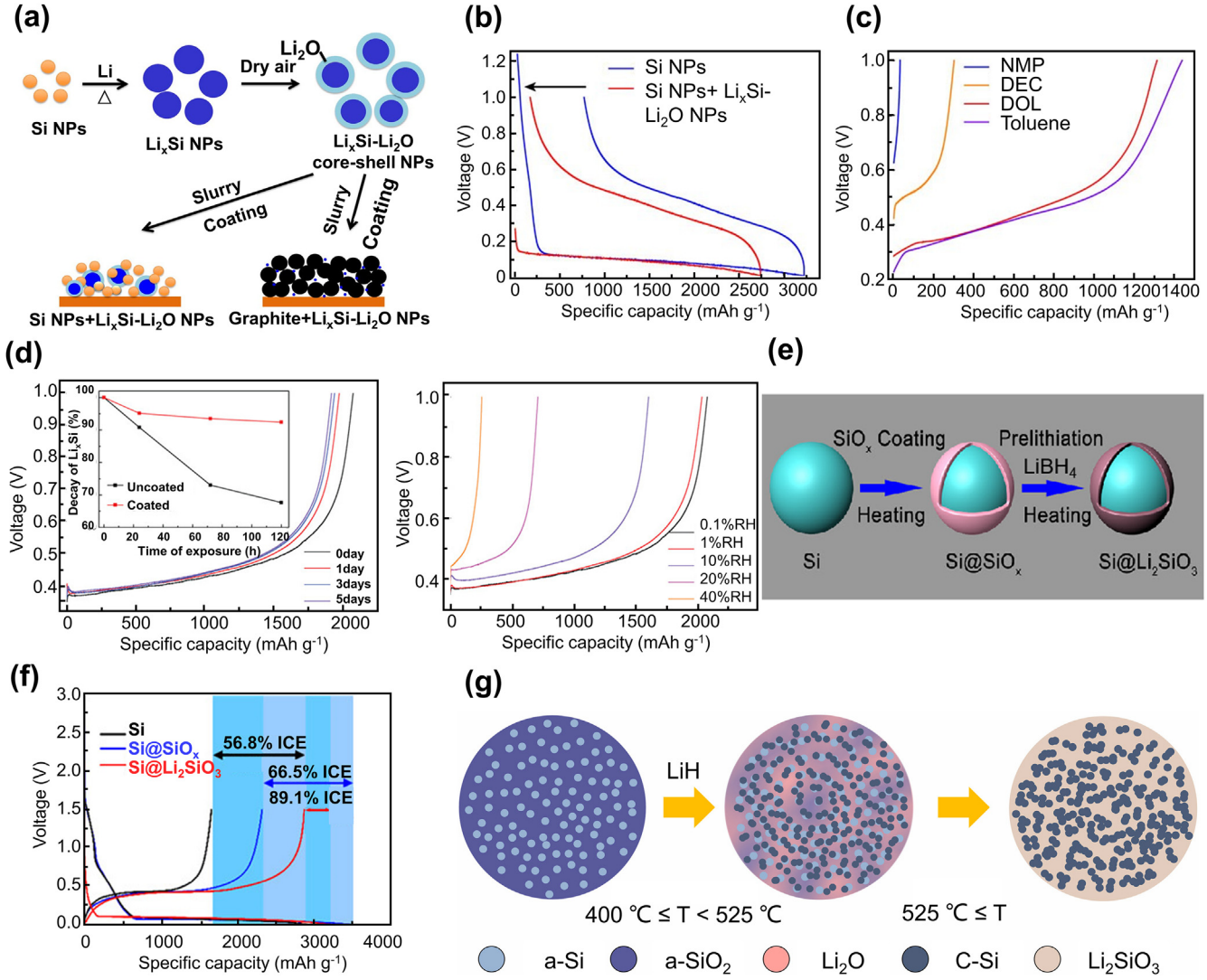

Fig. 7. (a) Thermal alloying process of synthesizing lithiated active materials Li_xSi–Li_2O core–shell NPs, and the application in anodes. Reprinted with permission from Ref. [103]. Copyright (2014) Springer Nature. (b) First cycle voltage profiles of Si NPs (nanoparticles) and Si NPs with lithiated Li_xSi–Li_2O NPs active materials. The ICE was significantly improved after adding LixSi–Li_2O NPs to Si NPs. Reprinted with permission from Ref. [103]. Copyright (2014) Springer Nature. (c) First delithiation specific capacity of Li_xSi–Li_2O NPs in different solvents: N-methyl-2-pyrrolidone (NMP), diethyl carbonate (DEC), 1,3-dioxolane (DOL) and toluene. Reprinted with permission from Ref. [103]. Copyright (2014) Springer Nature. (d) Delithiation capacity of coated LixSi exposed to dry air for different periods (0 day-5 days). The inset figure shows the dependence of decay rate on exposure time. Reprinted with permission from Ref. [104]. Copyright (2015) American Chemical Society. (e) Process of producing Si@SiOx particle, and Si@Li_2SiO_3 particle using $LiBH_4$. Reprinted with permission from Ref. [105]. Copyright (2019) American Chemical Society. (f) First cycle lithiation/delithiation curve of Si, Si@SiOx, Si@Li_2SiO_3 electrodes show that ICE of Si@Li_2SiO_3 is the highest. Reprinted with permission from Ref. [105]. Copyright (2019) American Chemical Society. (g) Chemical reaction mechanism of LiH and SiO at high temperature. Reprinted with permission from Ref. [106]. Copyright (2021) Elsevier.

which reduced the consumption of lithium ions in the electrolyte during the first cycle, and Li_xSiO_y material also ensured the structural integrity of SiO_x/C particles. However, Li–biphenyl (BP) and Li–naphthalene (NP) are not perfect for chemical prelithiating silicon-based materials, although they worked effectively for graphite.

As shown in Fig. 8b, the potentials of Li-BP (0.33 V) and Li-NP (0.37 V) are higher than that of Si-based material (~0.29 V). Therefore, the above reagents are not suitable to chemically lithiate silicon-based electrodes but rather form SEI [110]. Electrical wiring between SiO_x electrodes and Li through conductive Li–arene (i.e. aromatic hydrocarbon) complex (LAC) solutions allows lithiation of SiO_x, but such reactions require a reaction time of several days or a micrometer-level distance between Li and the electrode to offset the resistance of the solutions, which counters the benefits of the chemical prelithiation strategy. Chemical reagents with sufficient reducing strength are required to accomplish chemical prelithiation of Si-based anode. Jang et al. [110] found that the position and number of methyl groups on the biphenyl were directly correlated with the electrochemical potential. Compared with BP, NP, 2-methyl BP, 3,3′-dimethyl BP, and 4,4′-dimethyl BP, Li-3,3′,4,4′-tetramethyl BP (3,3′,4,4′-TMBP), as shown in Fig. 8b, had quite low potential of 0.33 V,

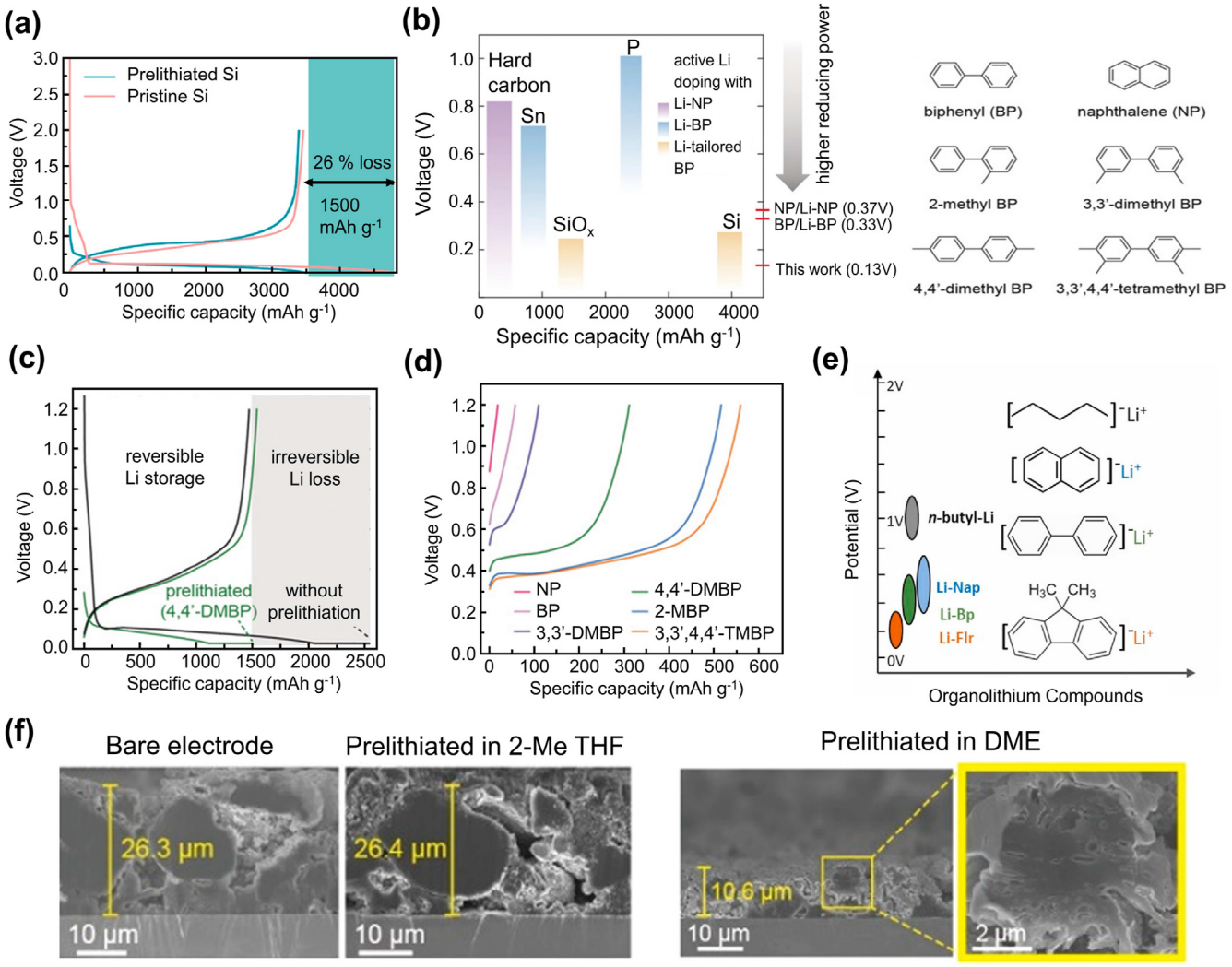

Fig. 8. (a) First cycle charge/discharge profiles of pristine Si and prelithiated Si. Reprinted with permission from Ref. [108]. Copyright (2019) American Chemical Society. (b) Capacities and potentials of hard carbon chemically prelithiated with Li-NP, Sn and P chemically prelithiated with Li-BP, SiOx and Si chemically prelithiated with Li-tailored BP NP (left). Molecular structures of BP, NP, 2-methyl BP, 3,3′-dimethyl BP, 4,4′-dimethyl BP and 3,3′,4,4′-dimethyl BP (right). Reprinted with permission from Ref. [110]. Copyright (2020) John Wiley and Sons. (c) First cycle charge/discharge profiles of SiOx electrodes with (green curve) and without (black curve) prelithiation. Reprinted with permission from Ref. [110]. Copyright (2020) John Wiley and Sons. (d) Delithiation capacities of SiOx electrodes chemically prelithiated with NP and BP derivatives. Reprinted with permission from Ref. [110]. Copyright (2020) John Wiley and Sons. (e) Potentials and structures of n-butyl-Li, Li-NP, Li-BP and Li–FIr chemical prelithiation regents. Reprinted with permission from Ref. [111]. Copyright (2020) Elsevier. (f) Cross-sectioned SEM images of pristine electrode, prelithiated using 2-meTHF and DME as solvents. Reprinted with permission from Ref. [112]. Copyright (2021) American Chemical Society.

0.37 V, 0.131 V, 0.294 V, 0.186 V, respectively. The ICE can be sufficiently increased when 4,4′-dimethyl BP was used as the prelithiated reagents (Fig. 8c). The delithiation capacities of the SiO_x electrodes immersed in lithium–arene complex (LAC) solutions of 3,3′,4,4′-TMBP was 560 mAh g^{-1}, which was the best among the LACs and equivalent to 37% of the reversible capacity of SiO_x (Fig. 8d). Zhang et al. [111] reported a new organolithium compound, i.e. Li-9,9-dimethyl-9H-fluorene-tetrahydrofuran (FIr), with a low redox potential of ~0.18 V and strong reducing power to prelithiate SiO-based anode (Fig. 8e). Compared to Li-NP and Li-BP, which take hours to incompletely lithiate the anode, Li–FIr can efficiently chemical lithiate SiO in minutes due to fast electron and lithium migration from FIr to Si-based materials. What's more, the prelithiation by Li–FIr was more complete than that by Li-NP and Li-BP and it successfully alleviated lithium loss during cycling.

Beside the organolithium compounds, the selection of solvents which affects the solvation/desolvation process is another key to the chemical prelithiation process. Ether solvents such as THF and DME have been widely used for LAC solutions, whereas carbonate solvents are excluded because arene radical anions reduce most carbonate solvents [112]. In order to achieve the robust prelithiation of anodes, it is necessary to destabilize the solvated ions and stabilize the Li^+-organic anion contact ion pairs during the desolvation process by tailoring the solvation power of solvents. Simply immersing the anode in weakly solvating LAC solutions significantly improved the ICE in which the Li^+-BP radical anion bond was maintained until the complete de-coordination of the Li^+ ion in weak solvents. Choi et al. [112] revealed that it was better to

use weakly solvating solutions like tetrahydrofuran (THF), 2-methylte-trahydrofuran (2-meTHF) and tetrahydropyran (THP), as the solvents than strongly solvating solvents like 1,2-dimethoxyethane (DME) and diglyme (DEGDME), since lithium ions tend to combine with negative ion (BP^-) to form contact ion pairs (CIPs) and aggregated ion pairs (AIPs) in weakly solvating solution. The prelihtiated Si-based electrodes in DME were damaged because the solvated ions formed by lithium ions and DME embedded themselves into the silicon-based material, destroying the structure of the particles (Fig. 8f), which did not happen in the 2-meTHF or THP case. According to ionic solvation and coordination chemistry, Shen et al. [113] also selected the strong electron-donating, sterically hindered and chemically stable solvent (2-meTHF) to dissolve biphenyl and lithium metal and realized efficient chemical prelithiation to significantly improve the ICE and energy densities of the anodes.

Chemical prelithiation is a mild, practical and simple method. Solution used in chemical prelithiation is stable in air, the efficiency is very high and the prelithiation is homogeneous. There is increasing attention on this field given its simplicity, and chemical prelithiation is promising to realize a feasible roll-to-roll prelithiation process that could be adopted by industry. However, for silicon-based materials, the redox potentials of most Li-arene complexes are too high to drop lithium ions into silicon-based materials. The cost of the organolithium compounds and their solution, handling of the chemicals with high reactivity, etc. are still problematic for commercial production.

4. Summary and perspectives

In this review, the challenges of silicon-based materials, including volume expansion, particle rupture and pulverization and low ICE etc., were introduced. The origin of lithium loss and the necessity of prelithiation of silicon-based materials were addressed. The severe active lithium loss, originating from SEI formation, volumetric changes and defect sites, is one of the primary drawbacks for silicon-based materials, hindering its practical development and application. In order to offset active lithium loss, various prelithiation methods have been developed, including electrochemical method, direct contact method, active material assisted method, chemical method. The principles and applications of these strategies are discussed in detail. These methods provide the promising potential for practical and large-scale application of silicon-based anodes to boost ICE and enhance the cycle performance of these materials. The progress brings up new insights into the application of prelithiation in silicon-based anodes. Although previous prelithiation reports can improve the ICE to some extent, there are still some issues to be resolved for silicon-based materials, such as poor electrical conductivity, inferior rate capacity and severe interfacial side reactions. It would be valuable if the prelithiation technology can not only compensates the active lithium loss but also addresses the above-mentioned problems in the next generation silicon-based high energy density LIBs.

Despite all the progress, there are still a lot of challenges as addressed above and more investigations are still highly desired to assess the significance of prelithiation strategies for the next generation commercial LIBs. The following aspects need to be further addressed for future studies on the prelithiation of silicon-based anode materials. (1) The processes of most prelithiation methods are complex and high-cost, which is quite hard to realize in large-scale production. Convenient and economical method still needs to be developed. (2) The rapid development of novel silicon-based anode materials demand for corresponding prelithiation strategies to inherently improve their coulombic efficiency, cycling stability and lifetime. It would be a key to select the proper prelithiation method for a specific anode material according to its intrinsic property. (3) So far, the prelithiation cannot be well controlled, especially in direct contact methods. Many of the current study on prelithiation focus on the key experimental parameters of prelithiation, however the reaction mechanism during prelithiation process and the corresponding effects are still not fully understood. Only with a fully understanding of the prelithiation mechanism, the reduction of active lithium loss and improvement of recycling capacity can be manageable. (4) Establishing stable, robust, and homogeneous SEI on the surface of silicon-based materials by prelithiation is also promising in addition to compensating for active lithium loss. (5) The exploration of lithium-arene complexes with lower redox potential which are appropriate for various anodes' chemical prelithiation would be very meaningful. (6) Furthermore, compatibility and safety consideration of prelithiation are essential in commercial cell fabrication. The manipulation and optimization of prelithiation technology would be significant before its commercialization.

Conflict of interest

The authors declare that they have no known competing financial interests or personal relationships that could have appeared to influence the work reported in this paper.

Acknowledgements

This work was supported by Guangdong Basic and Applied Basic Research Foundation (2019A1515110530, 2022A1515010486), Shenzhen Science and Technology Program (JCYJ20210324140804013), and Tsinghua Shenzhen International Graduate School (QD2021005N, JC2021007).

References

[1] H. Ouyang, S. Min, J. Yi, X. Liu, F. Ning, J. Qin, Y. Jiang, B. Zhao, J. Zhang, Green Energy Environ. 8 (2023) 1195–1204.
[2] Y. Wang, W. Pan, K.W. Leong, Y. Zhang, X. Zhao, S. Luo, D.Y.C. Leung, Green Energy Environ. (2021), https://doi.org/10.1016/j.gee.2021.10.001.
[3] Z. Wang, K. Zhang, B. Zhang, Z. Tong, S. Mao, H. Bai, Y. Lu, Green Energy Environ. 7 (2022) 1401–1410.
[4] Y. Lv, S. Huang, S. Lu, W. Ding, X. Yu, G. Liang, J. Zou, F. Kang, J. Zhang, Y. Cao, J. Power Sources 536 (2022) 231510.

[5] N. Li, T. Jia, Y. Liu, S. Huang, F. Kang, Y. Cao, Front. Chem. 10 (2022) 884308.
[6] L. Lu, X. Han, J. Li, J. Hua, M. Ouyang, J. Power Sources 226 (2013) 272–288.
[7] S. Choi, G. Wang, Adv. Mater. Tech. 3 (2018) 1700376.
[8] M. Li, J. Lu, Z. Chen, K. Amine, Adv. Mater. 30 (2018) e1800561.
[9] Z. Zheng, H. Gao, C. Ke, M. Li, Y. Cheng, D.L. Peng, Q. Zhang, M.S. Wang, ACS Appl. Mater. Interfaces 13 (2021) 53818–53828.
[10] G.M. Veith, M. Doucet, R.L. Sacci, B. Vacaliuc, J.K. Baldwin, J.F. Browning, Sci. Rep. 1 (2017) 1–15.
[11] D.H. Tan, Y.T. Chen, H. Yang, W. Bao, B. Sreenarayanan, J.M. Doux, W. Li, B. Lu, S.Y. Ham, B. Sayahpour, Science 373 (2021) 1494–1499.
[12] W. An, B. Gao, S. Mei, B. Xiang, J. Fu, L. Wang, Q. Zhang, P.K. Chu, K. Huo, Nat. Commun. 10 (2019) 1–11.
[13] Y. Yang, S. Liu, X. Bian, J. Feng, Y. An, C. Yuan, ACS Nano 12 (2018) 2900–2908.
[14] L. Chen, Y. Weng, Y. Meng, F. Dou, Z. An, P. Song, G. Chen, D. Zhang, ACS Appl. Energy Mater. 3 (2020) 9337–9347.
[15] X. Wu, X. Lan, R. Hu, Y. Yao, Y. Yu, M. Zhu, Adv. Mater. 34 (2021) e2106895.
[16] P. Nithyadharseni, M.V. Reddy, B. Nalini, M. Kalpana, B.V.R. Chowdari, Electrochim. Acta 161 (2015) 261–268.
[17] A. Varzi, L. Mattarozzi, S. Cattarin, P. Guerriero, S. Passerini, Adv. Energy Mater. 8 (2018) 1701706.
[18] Z. Liu, X. Luo, L. Qin, G. Fang, S. Liang, Adv. Powder Mater. 1 (2022) 100011.
[19] A. Magasinski, P. Dixon, B. Hertzberg, A. Kvit, J. Ayala, G. Yushin, Nat. Mater. 9 (2010) 353–358.
[20] M.N. Obrovac, Curr. Opin. Electrochem. 9 (2018) 8–17.
[21] Y. Cao, T.D. Hatchard, R.A. Dunlap, M.N. Obrovac, J. Mater. Chem. A 7 (2019) 8335–8343.
[22] Y. Cao, S. Hans, J. Liese, U. Werner-Zwanziger, J. Wang, J.C. Bennett, R.A. Dunlap, M.N. Obrovac, Chem. Mater. 33 (2021) 7386–7395.
[23] C.L. Berhaut, D.Z. Dominguez, D. Tomasi, C. Vincens, C. Haon, Y. Reynier, W. Porcher, N. Boudet, N. Blanc, G.A. Chahine, S. Tardif, S. Pouget, S. Lyonnard, Energy Storage Mater. 29 (2020) 190–197.
[24] C. Zhang, F. Wang, J. Han, S. Bai, J. Tan, J. Liu, F. Li, Small Structures 2 (2021) 2100009.
[25] J. Entwistle, Energy Rep. 6 (2020) 225–231.
[26] H. Tian, H. Tian, W. Yang, F. Zhang, W. Yang, Q. Zhang, Y. Wang, J. Liu, S.R.P. Silva, H. Liu, G. Wang, Adv. Funct. Mater. 31 (2021) 2101796.
[27] K. Schroder, J. Alvarado, T.A. Yersak, J. Li, N. Dudney, L.J. Webb, Y.S. Meng, K.J. Stevenson, Chem. Mater. 27 (2015) 5531–5542.
[28] C. Cao, I.I. Abate, E. Sivonxay, B. Shyam, C. Jia, B. Moritz, T.P. Devereaux, K.A. Persson, H.-G. Steinrück, M.F. Toney, Joule 3 (2019) 762–781.
[29] K. Guo, R. Kumar, X. Xiao, B.W. Sheldon, H. Gao, Nano Energy 68 (2020) 104257.
[30] C. Stetson, Y. Yin, A. Norman, S.P. Harvey, M. Schnabel, C. Ban, C.-S. Jiang, S.C. DeCaluwe, M. Al-Jassim, J. Power Sources 482 (2021) 228946.
[31] Z. Zhang, Y. Li, R. Xu, W. Zhou, Y. Li, S.T. Oyakhire, Y. Wu, J. Xu, H. Wang, Z. Yu, D.T. Boyle, W. Huang, Y. Ye, H. Chen, J. Wan, Z. Bao, W. Chiu, Y. Cui, Science 375 (2022) 66–70.
[32] W. He, H. Tian, F. Xin, W. Han, J. Mater. Chem. A 3 (2015) 17956–17962.
[33] H. Song, H.X. Wang, Z. Lin, X. Jiang, L. Yu, J. Xu, Z. Yu, X. Zhang, Y. Liu, P. He, L. Pan, Y. Shi, H. Zhou, K. Chen, Adv. Funct. Mater. 26 (2016) 524–531.
[34] J. Su, C. Zhang, X. Chen, S. Liu, T. Huang, A. Yu, J. Power Sources 381 (2018) 66–71.
[35] Q. Zhang, H. Chen, L. Luo, B. Zhao, H. Luo, X. Han, J. Wang, C. Wang, Y. Yang, T. Zhu, M. Liu, Energy Environ. Sci. 11 (2018) 669–681.
[36] H. Li, H. Li, Y. Lai, Z. Yang, Q. Yang, Y. Liu, Z. Zheng, Y. Liu, Y. Sun, B. Zhong, Adv. Energy Mater. 7 (2022) 2102181.
[37] H. Chen, X. Hou, F. Chen, S. Wang, B. Wu, Q. Ru, H. Qin, Y.J.C. Xia, Carbon 130 (2018) 433–440.
[38] G. Huang, J. Han, Z. Lu, D. Wei, H. Kashani, K. Watanabe, M. Chen, ACS Nano 14 (2020) 4374–4382.
[39] W. An, P. He, Z. Che, C. Xiao, E. Guo, C. Pang, X. He, J. Ren, G. Yuan, N. Du, D. Yang, D.L. Peng, Q. Zhang, ACS Appl. Mater. Interfaces 14 (2022) 10308–10318.
[40] Y. Yao, N. Liu, M.T. McDowell, M. Pasta, Y. Cui, Energy Environ. Sci. 5 (2012) 7927–7930.
[41] F. Wang, G. Chen, N. Zhang, X. Liu, R. Ma, Carbon Energy 1 (2019) 219–245.
[42] D. Kim, K.H. Kim, C. Lim, Y. Lee, Carbon Energy 1 (2022) 321–328.
[43] X. Han, Z. Zhang, H. Chen, L. Luo, Q. Zhang, J. Chen, S. Chen, Y. Yang, J. Mater. Chem. A 9 (2021) 3628–3636.
[44] Y. Zeng, Y. Huang, N. Liu, X. Wang, Y. Zhang, Y. Guo, H.-H. Wu, H. Chen, X. Tang, Q. Zhang, J. Energy Chem. 54 (2021) 727–735.
[45] C. Ke, F. Liu, Z. Zheng, H. Zhang, M. Cai, M. Li, Q. Yan, H. Chen, Q. Zhang, Rare Metals. 40 (2021) 1347–1356.
[46] M. Jiao, Y. Wang, C. Ye, C. Wang, W. Zhang, C. Liang, J. Alloys Compd. 842 (2020) 155774.
[47] Y. Cao, R. Dunlap, R. Obrovac, J. Electrochem. Soc. 167 (2020) 110501.
[48] Y. Li, Y. Qian, J. Zhou, N. Lin, Y. Qian, Nano Res. 15 (2021) 230–237.
[49] X. Zhang, H. Qu, W. Ji, D. Zheng, T. Ding, C. Abegglen, D. Qiu, D. Qu, ACS Appl. Mater. Interfaces 12 (2020) 11589–11599.
[50] F. Holtstiege, P. Bärmann, R. Nölle, M. Winter, T. Placke, Batteries 4 (2018) 4.
[51] Y. Zhang, B. Wu, G. Mu, C. Ma, D. Mu, F. Wu, J. Energy Chem. 64 (2022) 615–650.
[52] L. Jin, C. Shen, Q. Wu, A. Shellikeri, J. Zheng, C. Zhang, J.P. Zheng, Adv. Sci. 8 (2021) e2005031.
[53] F. Wang, B. Wang, J. Li, B. Wang, Y. Zhou, D. Wang, H. Liu, S. Dou, ACS Nano 15 (2021) 2197–2218.
[54] K. Zou, W. Deng, P. Cai, X. Deng, B. Wang, C. Liu, J. Li, H. Hou, G. Zou, X. Ji, Adv. Funct. Mater. 31 (2020) 2005581.
[55] W. Bao, C. Fang, D. Cheng, Y. Zhang, B. Lu, D.H.S. Tan, R. Shimizu, B. Sreenarayanan, S. Bai, W. Li, M. Zhang, Y.S. Meng, Cell Rep. Phys. Sci. 2 (2021) 100597.
[56] K.H. Kim, J. Shon, H. Jeong, H. Park, S.J. Lim, J.S. Heo, J. Power Sources 459 (2020) 228066.
[57] S.K. Heiskanen, J. Kim, B.L. Lucht, Joule 3 (2019) 2322–2333.
[58] A. Ramasubramanian, V. Yurkiv, T. Foroozan, M. Ragone, R. Shahbazian-Yassar, F. Mashayek, J. Phys. Chem. C 123 (2019) 10237–10245.
[59] T. Ortner, Commun. Chem. 4 (2021) 1–2.
[60] A.L. Michan, M. Leskes, C. Grey, Chem. Mater. 28 (2016) 385–398.
[61] H. Steinrück, C. Cao, G.M. Veith, M. Toney, J. Chem. Phys. 152 (2020) 084702.
[62] D. Rehnlund, F. Lindgren, S. Böhme, T. Nordh, Y. Zou, J. Pettersson, U. Bexell, M. Boman, K. Edström, L. Nyholm, Science 10 (2017) 1350–1357.
[63] B. Zhu, G. Liu, G. Lv, Y. Mu, Y. Zhao, Y. Wang, X. Li, P. Yao, Y. Deng, Y. Cui, Sci. Adv. 5 (2019) eaax0651.
[64] K. Ogata, E. Salager, C. Kerr, A. Fraser, C. Ducati, A.J. Morris, S. Hofmann, C. Grey, Nat. Commun. 5 (2014) 1–11.
[65] A.L. Michan, G. Divitini, A.J. Pell, M. Leskes, C. Ducati, C. Grey, J. Am. Chem. Soc. 138 (2016) 7918–7931.
[66] W. Bao, C. Fang, D. Cheng, Y. Zhang, B. Lu, D.H. Tan, R. Shimizu, B. Sreenarayanan, S. Bai, W. Li, Cell Rep. Phys. Sci. 2 (2021) 100597.
[67] J.S. Edge, S. O'Kane, R. Prosser, N.D. Kirkaldy, A.N. Patel, A. Hales, A. Ghosh, W. Ai, J. Chen, J. Jiang, Phys. Chem. Chem. Phys. 23 (2021) 8200–8221.
[68] J. Chen, X. Fan, Q. Li, H. Yang, M.R. Khoshi, Y. Xu, S. Hwang, L. Chen, X. Ji, C. Yang, H. He, C. Wang, E. Garfunkel, D. Su, O. Borodin, C. Wang, Nat. Energy 5 (2020) 386–397.
[69] Z. Cao, X. Zheng, Q. Qu, Y. Huang, H. Zheng, Adv. Mater. 33 (2021) e2103178.
[70] H. Chen, Y. Yang, D.T. Boyle, Y.K. Jeong, R. Xu, L.S. de Vasconcelos, Z. Huang, H. Wang, H. Wang, W. Huang, H. Li, J. Wang, H. Gu,

R. Matsumoto, K. Motohashi, Y. Nakayama, K. Zhao, Y. Cui, Nat. Energy 6 (2021) 790–798.
[71] X. Zhang, D. Wang, X. Qiu, Y. Ma, D. Kong, K. Müllen, X. Li, L. Zhi, Nat. Commun. 11 (2020) 1–9.
[72] Z. Zhang, H. Wang, M. Cheng, Y. He, X. Han, L. Luo, P. Su, W. Huang, J. Wang, C. Li, Energy Storage Mater. 42 (2021) 231–239.
[73] H.J. Kim, S. Choi, S.J. Lee, M.W. Seo, J.G. Lee, E. Deniz, Y.J. Lee, E.K. Kim, J.W. Choi, Nano Lett. 16 (2016) 282–288.
[74] H. Zhou, X. Wang, D. Chen, ChemSusChem 8 (2015) 2737–2744.
[75] L. Guo, C. Xin, J. Gao, J. Zhu, Y. Hu, Y. Zhang, J. Li, X. Fan, Y. Li, H. Li, Angew. Chem. Int. Ed. 133 (2021) 13123–13130.
[76] G.M. Overhoff, R. Nölle, V. Siozios, M. Winter, T. Placke, Batteries Supercaps 4 (2021) 1163–1174.
[77] S.A. Delp, O. Borodin, M. Olguin, C.G. Eisner, J.L. Allen, T. Jow, Electrochim. Acta 209 (2016) 498–510.
[78] Q. Meng, G. Li, J. Yue, Q. Xu, Y.X. Yin, Y.G. Guo, ACS Appl. Mater. Interfaces 11 (2019) 32062–32068.
[79] Z. Cao, P. Xu, H. Zhai, S. Du, J. Mandal, M. Dontigny, K. Zaghib, Y. Yang, Nano Lett. 16 (2016) 7235–7240.
[80] C. Yao, X. Li, Y. Deng, Y. Li, P. Yang, S. Zhang, J. Yuan, R. Wang, Carbon 168 (2020) 392–403.
[81] L. Shi, Y. Liu, W. Wang, A. Wang, Z. Jin, F. Wu, Y. Yang, J. Alloys Compd. 723 (2017) 974–982.
[82] N. Liu, L. Hu, M.T. McDowell, A. Jackson, Y. Cui, ACS Nano 5 (2011) 6487–6493.
[83] T. Watanabe, T. Tsuda, N. Ando, S. Nakamura, N. Hayashi, N. Soma, T. Gunji, T. Ohsaka, F. Matsumoto, Electrochim. Acta 324 (2019) 134848.
[84] A. Shellikeri, V. Watson, D. Adams, E. Kalu, J. Read, T. Jow, J. Zheng, J. Zheng, J. Electrochem. Soc. 164 (2017) A3914.
[85] P. Bärmann, M. Diehl, L. Göbel, M. Ruttert, S. Nowak, M. Winter, T. Placke, J. Power Sources 464 (2020) 228224.
[86] C. Jarvis, M. Lain, M. Yakovleva, Y. Gao, J. Power Sources 162 (2006) 800–802.
[87] Y. Li, B. Fitch, Electrochem. Commun. 13 (2011) 664–667.
[88] B. Xiang, L. Wang, G. Liu, A. Minor, J. Electrochem. Soc. 160 (2013) A415.
[89] Q. Pan, P. Zuo, T. Mu, C. Du, X. Cheng, Y. Ma, Y. Gao, G. Yin, J. Power Sources 347 (2017) 170–177.
[90] T. Yang, P. Jia, Q. Liu, L. Zhang, C. Du, J. Chen, H. Ye, X. Li, Y. Li, T. Shen, Angew. Chem. Int. Ed. 130 (2018) 12932–12935.
[91] Z. Wang, Y. Fu, Z. Zhang, S. Yuan, K. Amine, V. Battaglia, G. Liu, J. Power Sources 260 (2014) 57–61.
[92] H. Zhao, Z. Wang, P. Lu, M. Jiang, F. Shi, X. Song, Z. Zheng, X. Zhou, Y. Fu, G. Abdelbast, Nano Lett. 14 (2014) 6704–6710.
[93] M. Marinaro, M. Weinberger, M. Wohlfahrt-Mehrens, Electrochim. Acta 206 (2016) 99–107.
[94] M.S. Tahir, M. Weinberger, P. Balasubramanian, T. Diemant, R.J. Behm, M. Linden, M. Wohlfahrt-Mehrens, Electrochim. Acta 5 (2017) 10190–10199.
[95] M. Bai, L. Yang, Q. Jia, X. Tang, Y. Liu, H. Wang, M. Zhang, R. Guo, Y. Ma, ACS Appl. Mater. Interfaces 12 (2020) 47490–47502.
[96] M.W. Forney, M.J. Ganter, J.W. Staub, R.D. Ridgley, B. Landi, Nano Lett. 13 (2013) 4158–4163.
[97] B. Huang, T. Huang, L. Wan, A. Yu, ACS Sustain. Chem. Eng. 9 (2021) 648–657.
[98] L. Liao, T. Ma, Y. Xiao, M. Wang, Y. Gao, T. Fang, J. Alloys Compd. 873 (2021) 159700.
[99] G. Ai, Z. Wang, H. Zhao, W. Mao, Y. Fu, R. Yi, Y. Gao, V. Battaglia, D. Wang, S. Lopatin, J. Power Sources 309 (2016) 33–41.
[100] K. Yao, R. Liang, J. Zheng, J. Electrochem. En. Conv. Stor. 13 (2016) 011004.
[101] P. Bärmann, M. Mohrhardt, J.E. Frerichs, M. Helling, A. Kolesnikov, S. Klabunde, S. Nowak, M.R. Hansen, M. Winter, T. Placke, Adv. Energy Mater. 11 (2021) 2100925.
[102] A. Veluchamy, C. Doh, D. Kim, J. Lee, D. Lee, K. Ha, H. Shin, B. Jin, H. Kim, S. Moon, C. Park, J. Power Sources 188 (2009) 574–577.
[103] J. Zhao, Z. Lu, N. Liu, H.W. Lee, M.T. McDowell, Y. Cui, Nat. Commun. 5 (2014) 5088.
[104] J. Zhao, Z. Lu, H. Wang, W. Liu, H.W. Lee, K. Yan, D. Zhuo, D. Lin, N. Liu, Y. Cui, J. Am. Chem. Soc. 137 (2015) 8372–8375.
[105] Y. Zhu, W. Hu, J. Zhou, W. Cai, Y. Lu, J. Liang, X. Li, S. Zhu, Q. Fu, Y. Qian, ACS Appl. Mater. Interfaces 11 (2019) 18305–18312.
[106] D.J. Chung, D. Youn, S. Kim, D. Ma, J. Lee, W.J. Jeong, E. Park, J. Kim, C. Moon, J. Lee, Nano Energy. 89 (2021) 106378.
[107] M. Scott, A. Whitehead, J. Owen, J. Electrochem. Soc. 145 (1998) 1506.
[108] Y. Shen, J. Zhang, Y. Pu, H. Wang, B. Wang, J. Qian, Y. Cao, F. Zhong, X. Ai, H. Yang, ACS Energy Lett. 4 (2019) 1717–1724.
[109] M.Y. Yan, G. Li, J. Zhang, Y.F. Tian, Y.X. Yin, C.J. Zhang, K.C. Jiang, Q. Xu, H.L. Li, Y.G. Guo, ACS Appl. Mater. Interfaces 12 (2020) 27202–27209.
[110] J. Jang, I. Kang, J. Choi, H. Jeong, K.W. Yi, J. Hong, M. Lee, Angew. Chem. Int. Ed. 59 (2020) 14473–14480.
[111] X. Zhang, H. Qu, W. Ji, D. Zheng, T. Ding, D. Qiu, D. Qu, J. Power Sources 478 (2020) 229067.
[112] J. Choi, H. Jeong, J. Jang, A.R. Jeon, I. Kang, M. Kwon, J. Hong, M. Lee, J. Am. Chem. Soc. 143 (2021) 9169–9176.
[113] Y. Shen, X. Shen, M. Yang, J. Qian, Y. Cao, H. Yang, Y. Luo, X. Ai, Adv. Funct. Mater. 31 (2021) 2101181.

Tianqi Jia got her B.E. from Henan University of Science and Technology, China in 2019. She is currently a graduate at Shenzhen International Graduate School, Tsinghua University. Her research interest is silicon-based anode.

Feiyu Kang got is PhD from The Hong Kong University of Science and Technology in 1997. He has been a visiting scholar at Hokkaido University, Japan. He works at Tsinghua University since 1988. Currently, he is a professor at Shenzhen International Graduate School, Tsinghua University. His research interest includes advanced carbon materials, electrochemical technology, ecomaterials, energy storage and conversion devices.

Yidan Cao got her from PhD from Tsinghua University, China in 2016. Afterwards, she worked at Dalhousie University as a Killam postdoctoral fellow from 2016 to 2019. She is currently an assistant professor at Shenzhen International Graduate School, Tsinghua University. Her research interest includes advanced energy storage materials and devices for next-generation battery technology, nanomaterials development and electrochemistry.